Final Report

John Anglo

August 31, 2012

1 Introduction

The motivation for this project was to find calibration sources for all-sky imagers that could readily be observed in the field. As they are visible in ASI data whenever the sky is clear, stars were selected for this task, though some difficulty was expected in observing stars through devices that were not designed nor meant for the observation of point sources.

Early stages of the project dealt with finding a means to track and record star brightness from ASI data, which was composed of arrays of minute average frames having associated metadata, including date and time information about the image frames. Using this information a procedure was developed to convert astronomical coordinate information to pixel location, accurately predicting the location of a star to be observed within a small pixel radius. The total pixel value of the star in question would then be recorded, then the process repeated for each frame in an array, for data collected over the course of a month, for numerous stars, for about twenty sites housing all-sky imagers.

On nights when stars were visible for significant lengths of time, star pixel values were found to follow well-defined curves consistent with known atmospheric extinction mechanisms that describe terrestrial measurements of star brightness as dependent on the position of a star in the sky, i.e. its zenith angle. This finding made it possible to extrapolate from the pixel count curves in order to find magnitude values comparable to catalogued values of the visual magnitudes of each star. The collected magnitudes of ten different stars exhibited a linear relationship with their catalogue values as expected, and were also found to be consistent between sites.

It was proposed that some inconsistencies in the previously-mentioned linear relationship could be attributed to differences in star colour. Visual magnitudes as recorded in catalogues are measured through a narrow-band filter in the visible range of light, while imager data is collected over a wider band without comparable filtering. Fully correcting for this difference in band width would have required an understanding of the emission spectrum of each recorded star, as well as the spectral sensitivity of the imager instruments. There was a shortage of readily available information on the latter, meaning this correction was not feasible for the given time frame. Instead, an attempt to bypass this issue was made with the assumption that stars having similar spectral type would have similar emission spectra, so that the imagers would react to those stars in the same manner. Grouping the stars by spectral type was therefore expected to produce separate, better-defined linear relationships with visual magnitude.

2 Star tracking and data collection

A star's position in the celestial sphere is commonly specified in the equatorial coordinate system. The coordinate system defines positions in terms of two coordinates, the right ascension and declination, in a frame that does not rotate with the Earth. Tracking a star's position over time at a given location on the Earth requires knowing these coordinates, the coordinates of the imager site and the time. With this information the star's zenith and azimuth angles, both locally-defined coordinates, can be determined.

In the case of tracking a star at a known right ascension and declination in ASI data frames, the location of the imager can be looked up without difficulty. Imager data files are processed into image arrays having associated metadata arrays; the time at which each image was taken is stored as part of the metadata. The zenith and azimuth angles are converted into pixel coordinates, using some parameters specific to individual imager sites: the ratio of pixel distance to angular distance, approximately 82.5 pixels per radian given that the boundaries of a circular image frame having a pixel size of 256×256 ideally coincide with the horizon around the instrument; the position of the zenith, expected to be near (128, 128); and a rotational offset dependent on the instrument's orientation relative to geographic north.

A one-time manual adjustment for each site of these parameters proved to remain reliable throughout the whole data set. Finding the exact position of a star using the tracking algorithm would then require looking for a maximum pixel value within a small radius of the coordinates predicted by the algorithm. Once a star was located, its pixel value would be recorded as the sum of the values within a small circle centred at the maximum point found, minus a background value found as the average value of pixels on the perimeter of the small circle. The corresponding zenith angle of the star would also be recorded.

This automated process allowed for the collection of a large amount of star data during off-hours: Over the course of the project, star data was collected for ten different stars - Capella, Procyon, Betelgeuse, Vega, Arcturus, Aldebaran, Deneb, Sirius, Rigel and Pollux - at twenty different imager sites, using ASI data recorded over the month of January 2011. Six of the sites having continuous periods of time in which stars were visible were selected for analysis.

3 Analysing star data

The aim at this point was to turn the star data into something that could be compared to values found in a catalogue. Pixel values were assumed to be linear in some manner to stellar flux, which in turn is logarithmically related to a star's magnitude. Meanwhile, the apparent curves followed by the pixel values consistently throughout clear nights were believed to be due to atmospheric extinction: A star's light has to travel some thickness of atmosphere to arrive at a terrestrial observer; the thickness increases with zenith angle z as a function of $\sec z$ for the small-z approximation, where the atmosphere is approximately flat and uniform. Some amount H is effectively removed from a star's magnitude by the atmosphere at the zenith, while $H \sec z$ is removed at an angle z. The quantity approximated here as $\sec z$ is known as the air mass.

Combining this information led to the hypothesis that pixel value y would be related

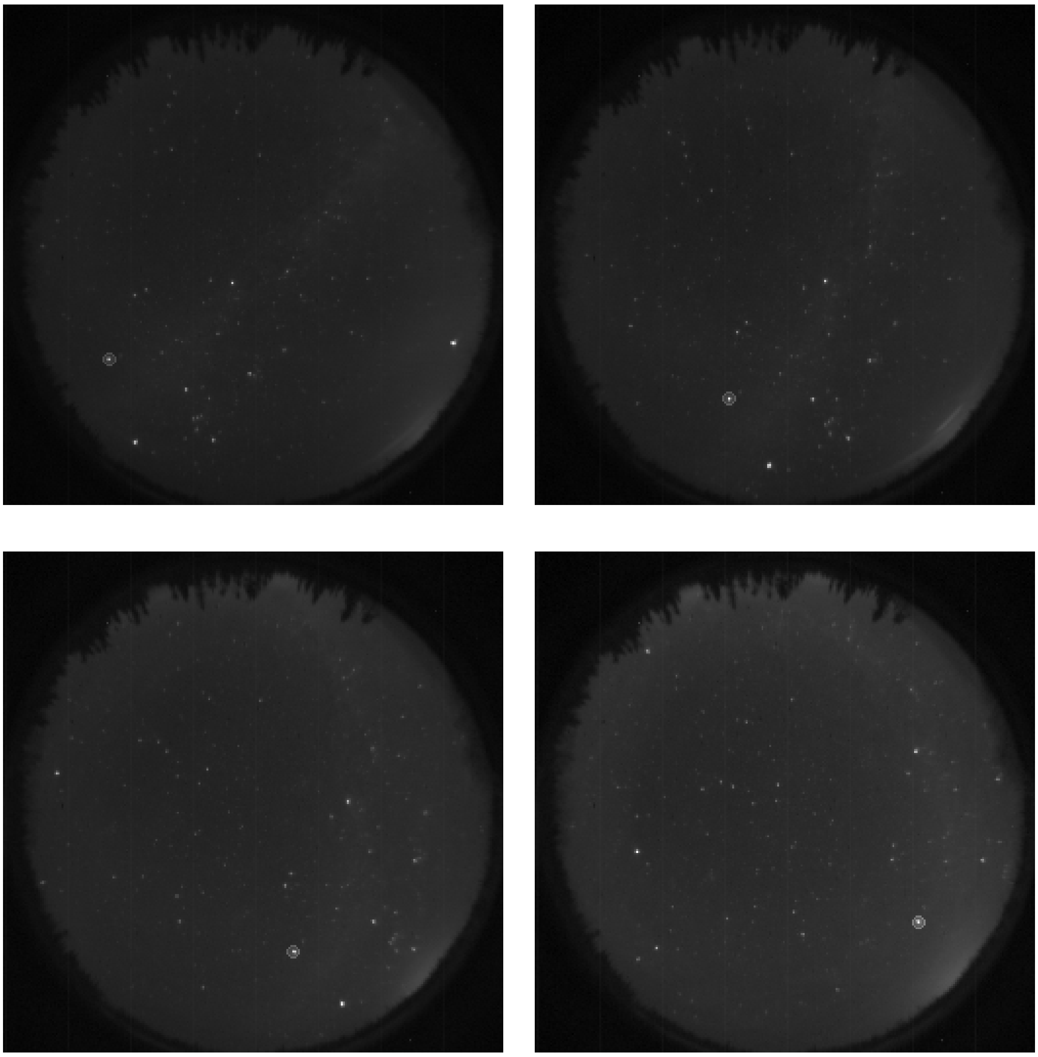

Figure 1: Sample images from a visualisation of the star tracking algorithm, for Procyon at The Pas on January 31, 2011. These images were captured every 120 frames. The highlighted circle of pixels around the star are used to find an average background value.

to zenith angle z by the equation

$$\log(y) = a + H \sec z. \tag{1}$$

Here $\log(y) = a$ without the value subtracted due to atmospheric extinction, implying that a is what the instrument would hypothetically measure if placed outside of the atmosphere, which means a should be linear with apparent visual magnitude.

The formula involving $\sec z$ is known to be reliable only up to about $z = 60°$, so to find a working relationship for as much data as possible required an equation incorporating an air mass formula that was accurate to larger zenith angles:

$$\log(y) = a + \frac{H}{\cos z + 0.025e^{-11\cos z}}. \tag{2}$$

Three predictions were made based on this equation: $\log(y)$ should be linear with $(\cos z + 0.025e^{-11\cos z})^{-1}$; as a coefficient describing local atmospheric conditions, H should remain roughly constant in a single night; finally, average values for a should be linear with and analogous to catalogue visual magnitudes, but with different scaling - by convention, the star magnitude scale places Vega at 0 magnitude and brightness increases as magnitude values become more negative, while a becomes more positive with brightness and has no definite zero point.

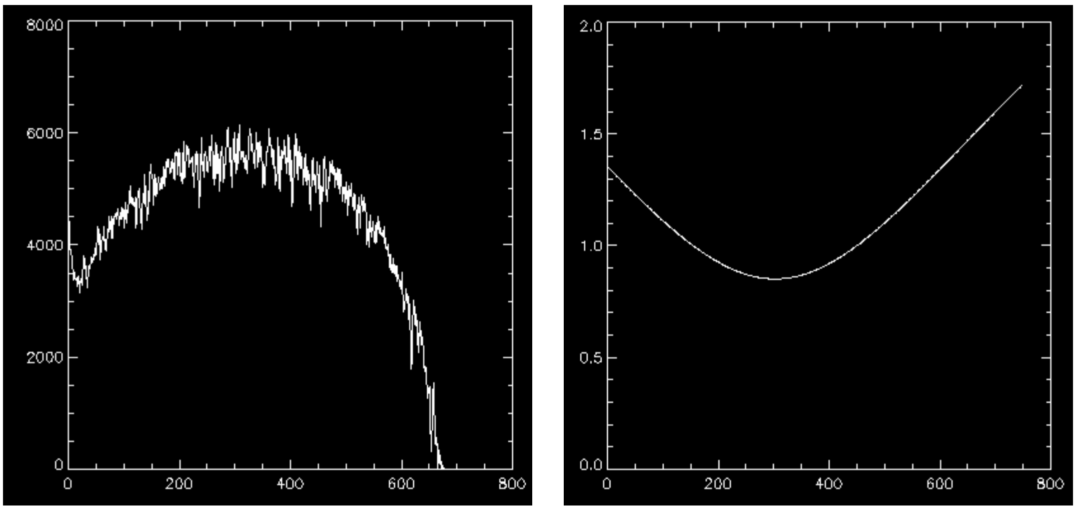

Figure 2: On the left, the total pixel value of Procyon over time at The Pas on January 31, 2011. On the right, the recorded zenith angle in radians.

Figures 2 and 3 show an example of data consistent with these predictions. In general, any series of clear star data would produce a curve much like that in Figure 2, and clear data was found to consistently produce reasonable linear fits as in Figure 3. Further, for five of the six sites selected for analysis, values of a for different stars were found to be similar, and within all six sites, the linear relationship between a and visual magnitudes appeared to have been confirmed as in Figure 4.

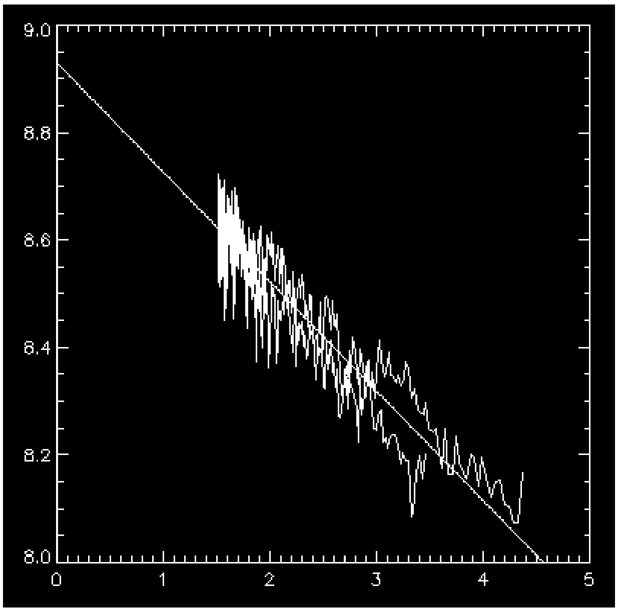

Figure 3: A plot of $\log(y)$ versus $(\cos z + 0.025e^{-11\cos z})^{-1}$ for the same data in Figure 2. The linear fit gives $a = 8.93 \pm 0.08$ for Procyon. The average value for Procyon measured at The Pas was $a = 8.92 \pm 0.05$, over eight nights of good visibility.

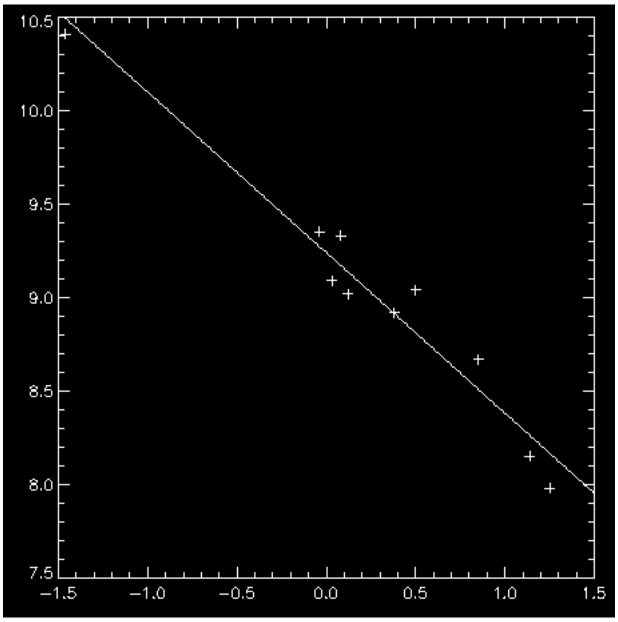

Figure 4: Average values of a for each of the ten stars surveyed at The Pas, plotted versus visual magnitude, and the resulting linear fit.

For a sixth site, Snap Lake, all values recorded were significantly lower than measured elsewhere. A reason for this discrepancy was not found during the course of analysis, but that the site data appears to be a lone anomaly suggests that the inconsistency is characteristic of the instrument.

4 Star colour considerations

Further analysis of the observations led to the realization that star data was colour-dependent, in a way that would make the direct comparison to visual magnitude performed previously, unreasonable. The imagers collect light from a wide band of wavelengths, and at varying sensitivities, while visual magnitude is measured through the narrow V filter, one of a set of three in the UBV photometric system commonly used in astronomical photometry.

Differences in the emission spectra of the different stars, combined with the instruments' variable sensitivity to different wavelengths of light, meant the magnitude values extracted from the star data would not exactly match visual magnitude values unless there was some means to extract stars' emissions within a narrow band comparable to that used to find visual magnitudes. While performing this correction would be a significant step towards using the data for absolute calibrations, doing so was not practicable at such a late stage into the project.

Instead, in order to reduce the variability of the emission spectra of the stars whose magnitudes were being compared, stars were grouped by similar spectral type with the belief that spectral type directly determined a star's emission spectrum, making it possible to assume that within each grouping, the instruments were responding to the different stars in much the same way. From the ten stars, two groups of four having similar spectral types were selected, as in Figures 5 and 6.

Differences in luminosity class (denoted by the Roman numeral after each alphanumeric spectral class) were largely ignored, as the values primarily describe widths of absorption lines in a star's spectrum. As the assumption held that the imagers collected light from a wide spectrum, approximating stars as black bodies, with spectra as smooth curves having no absorption lines, was deemed to be sufficient.

The more sparse selection of points available for comparison means more ideal linear correlations than that in Figure 4 are probable for the two sets of data, but less conclusive. Nonetheless, the groupings ensure to a degree that all of the information being compared in each plot is, in fact, theoretically compatible.

All magnitudes measured as in Section 3, along with plots like Figures 4 and 7, are collected in the spreadsheet `star-magnitudes.ods`, for all six sites surveyed.

5 Future work

As mentioned before, correcting for the imagers' sensitivity to different wavelengths of light seems to be a fundamental step towards absolute calibration, for which there was not enough time in the four-month project, and so here would be a reasonable place to

Name of star	Spectral type	Visual magnitude	Measured magnitude, a
Sirius	A1 V	-1.46	10.41
Rigel	B8 I	0.12	9.02
Vega	A0 V	0.03	9.09
Deneb	A2 I	1.25	7.98

Figure 5: A group of stars, selected for having spectral type of A0 or similar. Finding a grouping that incorporated Vega was fortunate, as A0 V stars like Vega are commonly used as calibration sources in astronomy. The fourth column lists the measured values from the linear interpolation from the previous section.

Name of star	Spectral type	Visual magnitude	Measured magnitude, a
Capella	G8	0.08	9.33
Arcturus	K1 III	-0.04	9.35
Aldebaran	K5 III	0.85	8.67
Pollux	K0 III	1.14	8.15

Figure 6: The second group of selected stars. In the same way that B-type stars can be similar to A-type stars, the G spectral type is similar to the K type, making Capella comparable to the other three stars in this grouping.

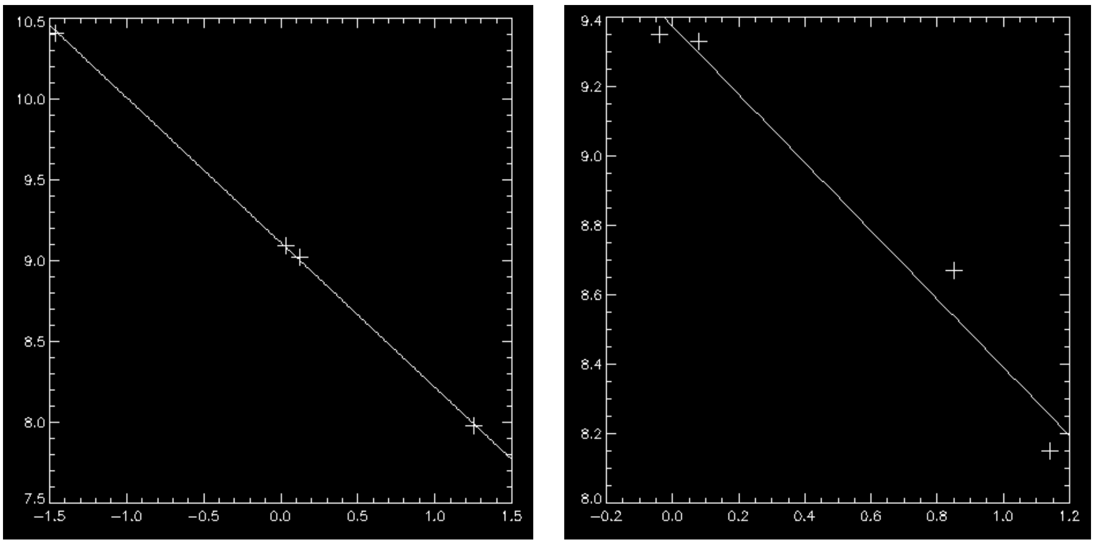

Figure 7: Average values of a measured at The Pas versus visual magnitude, in separate plots based on the data in Figures 5 and 6.

continue this particular line of work. One approach would be to use the various forms of information available in star catalogues, in conjunction with the visual magnitudes and spectral types used previously, to produce a clearer picture of star spectra over a wider range of wavelengths. In theory, knowing each star's black body temperature should suffice, if the end goal is an integrated value. On the instrument side, a function describing the imagers' relative response to various wavelengths is needed. Multiplying this function to the black body spectrum should give an accurate representation of a star's spectrum as an imager would see it, and integrating the value gives a magnitude over the same range of wavelengths, and with the same relative sensitivity, as the values extracted from the data.

However, all this is necessary if the only available data is monochromatic and unfiltered. Imager data gathered through numerous filters may allow for the construction of a spectrum from the data itself, provided that spectral sensitivity information is still available for the instruments. Theoretically, any set of narrow-band filters that cover the whole relevant range of wavelengths should produce a reasonable picture of a star spectrum, from which a slice could be taken at the V filter range - the filters used do not necessarily have to be the same filters used in conventional astronomy, i.e. in the UBV photometric system.

Outside of colour considerations, absolute calibration should be relatively straightforward. As a common calibration source in astronomical photometry, the flux spectrum of Vega has been measured and described intensively, which makes it a prime candidate for this calibration as well.

6 Conclusion

The successful extraction of star brightness information from ASI data, and the processing of said information into values comparable between sites independent of the sites' locations, suggest that bright stars produce enough information when photographed by all-sky imagers, to potentially be used as relative calibration sources in the field. The exercise of absolute calibration remains to be undertaken.

Given that the ideal form of absolute calibration would be the ability to directly relate stellar flux with pixel values in imager data, it does not seem to be possible to conclusively perform absolute calibration without first exploring the colour issue. However, past this issue, and with the combined methods used in relative calibration, complete absolute calibration should be a relatively simple task.